

Лекция 5.

Остывание одиночных компактных звёзд

1. Элементарная теория остывания белых карликов
2. Основные физические процессы, влияющие на остывание вырожденных звёзд
3. Реалистичные кривые остывания белых карликов
4. Тепловая структура остывающих нейтронных звёзд
5. Кривые остывания нейтронных звёзд
6. Об остывании кварковых звёзд

Остывание белого карлика

Простейшая модель [Mestel, *Mon. Not. R. astron. Soc.* **112**, 543 (1952)]:

$$T \frac{ds}{dt} = T \left(\frac{\partial s}{\partial T} \right)_{\rho} \frac{\partial T}{\partial t} + T \left(\frac{\partial s}{\partial \rho} \right)_{T} \frac{\partial \rho}{\partial t} = C_v \frac{\partial T}{\partial t} - \frac{T}{\rho^2} \left(\frac{\partial P}{\partial T} \right)_{\rho} \frac{\partial \rho}{\partial t}$$

$$L = - \int_0^M \frac{3}{2} \frac{k}{Am_p} \frac{\partial T_c}{\partial t} dM = - \frac{3}{2} \frac{kM}{Am_p} \frac{\partial T_c}{\partial t}$$

T_c – центральная (внутренняя) температура ~ температура на границе вырожденности.

Из оценки

$$T_6 \sim 8q^{2/7} \propto F_R^{2/7} \quad \text{где} \quad q = \frac{Z(1+Z)}{A} \frac{T_{e6}^4}{g_{14}}$$

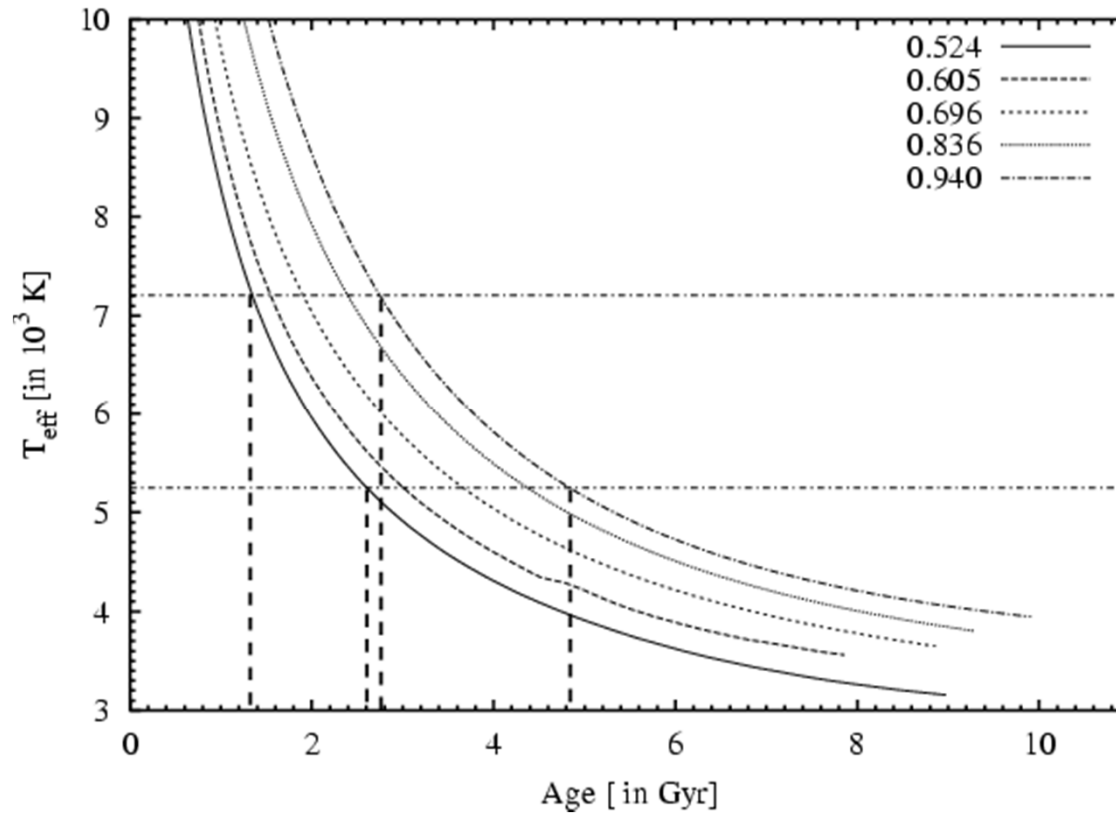
и $U \sim \frac{3}{2} k_B T \frac{M}{Am_u}$

получаем

$$\frac{dU}{dt} \propto L = 4\pi R^2 F_R \propto T^{7/2}$$
$$\Rightarrow T \propto t^{-2/5}$$

Остывание белого карлика

$$L \sim 8.4 \times 10^{-4} L_{\odot} \left(\frac{M}{M_{\odot}} \right) \left(\frac{t}{10^9 \text{ yrs}} \right)^{-7/5}$$

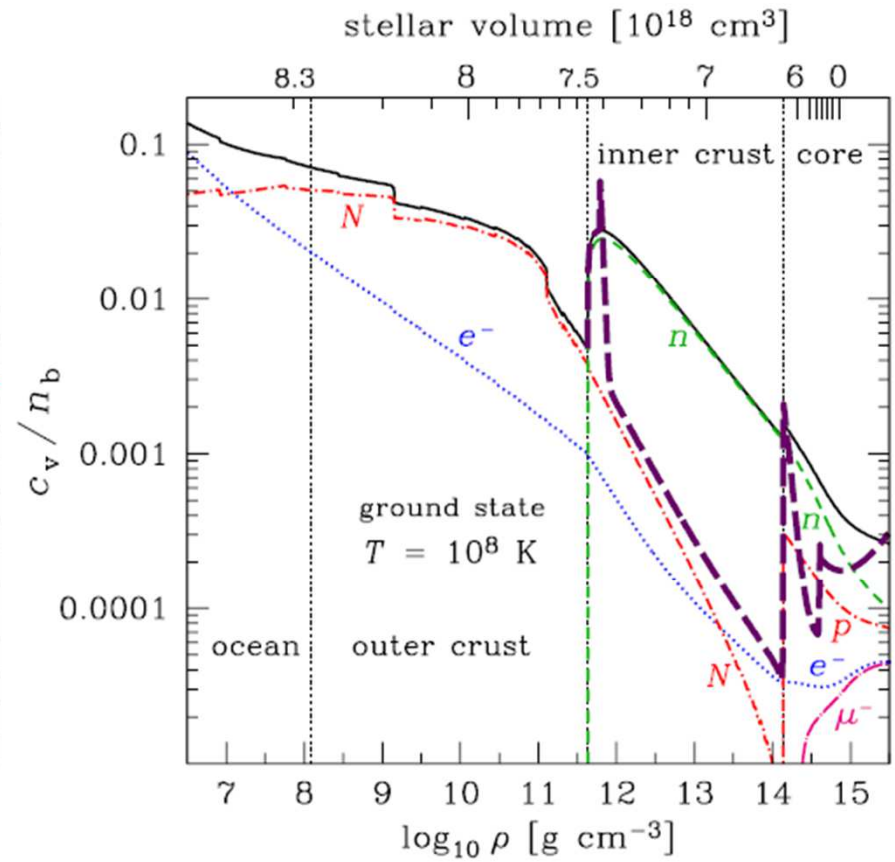
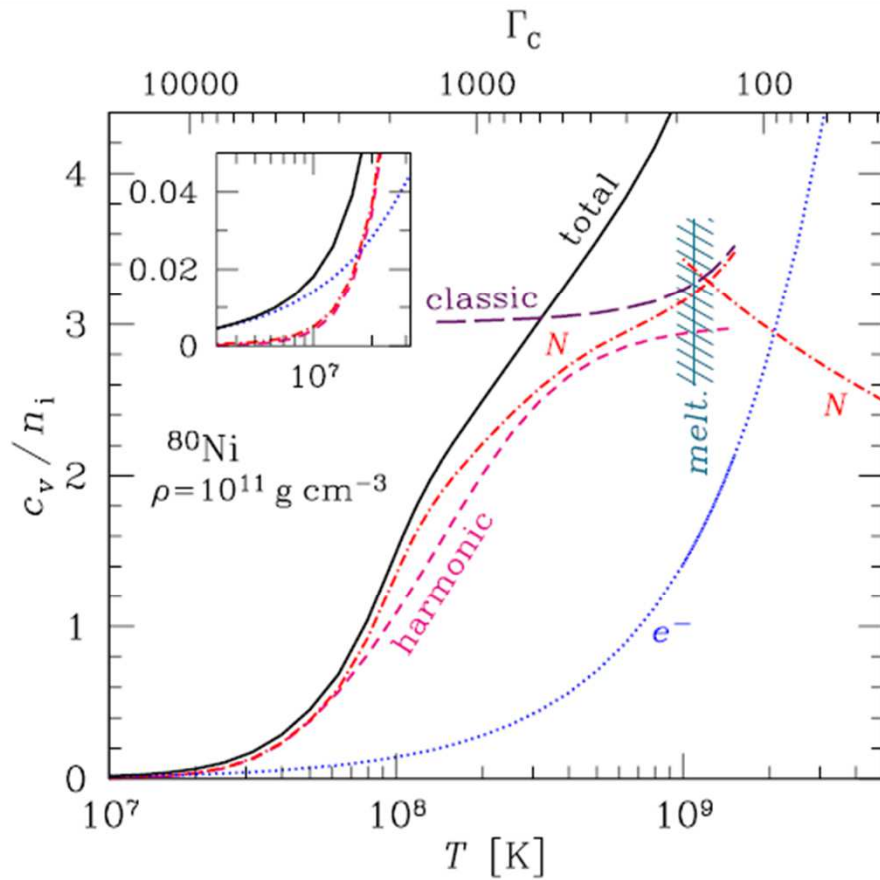


Теплоёмкость вырожденной плазмы

$$c_{v,e} = n_e \frac{\pi^2}{\rho_{\text{Fe}} c} T k_B^2 \gamma_r / x_r$$

$$c_{v,i} = \frac{3}{2} k_B n_i$$

$$c_{v,i}^{(D)} = n_i \frac{12\pi^4}{5} \left(\frac{T}{\Theta_D} \right)^3 k_B$$



Теплоёмкость вырожденной плазмы

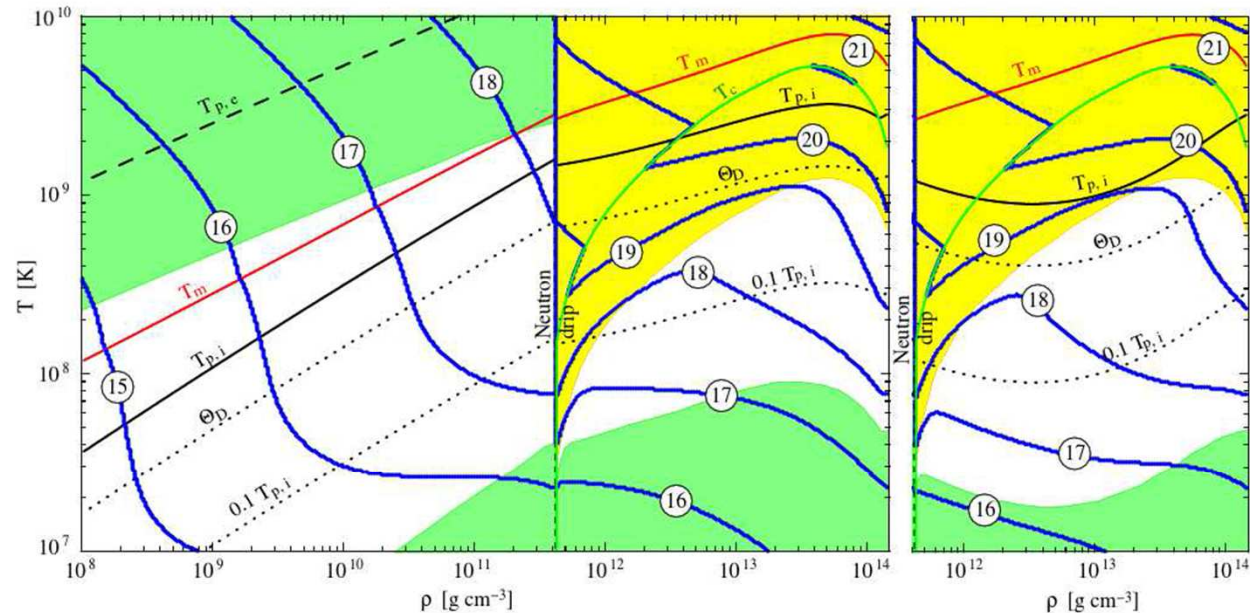


Fig. 2 Iso-contour lines of c_v in the crust, labeled by the value of $\log_{10}(c_v/\text{erg cm}^{-3} \text{K}^{-1})$. Also shown are the melting curve T_m and the critical temperature for neutron $^1\text{S}_0$ superfluidity, T_c , the electron and ion plasma temperatures, $T_{p,e}$ and T_p respectively, the Debye temperature, $\Theta_D \simeq 0.45T_p$, that marks the transition from classical to quantum solid and $0.1T_p$ below which the wholly quantum crystal regime is realized. The outer crust chemical composition is from [Haensel and Pichon \(1994\)](#) and inner crust from [Negele and Vautherin \(1973\)](#) with the neutron drip point at $\rho_{\text{drip}} = 4.3 \times 10^{11} \text{ g cm}^{-3}$. The electron contribution dominates in the two dark-shadowed (green) regions at high T and ρ below ρ_{drip} and at low T and high ρ , while neutrons dominate in the light-shadowed (yellow) region at high T and ρ above ρ_{drip} , and ions dominate in the intermediate regime. The right panel only displays the inner crust but assuming that about 80% of the dripped neutrons are entrained, illustrating the resulting increase in $c_{v,i}$, mainly due to the strong reduction of T_p and Θ_D , significantly extending the regime where $c_{v,i}$ dominates over $c_{v,e}$.

Теплопроводность вырожденной плазмы

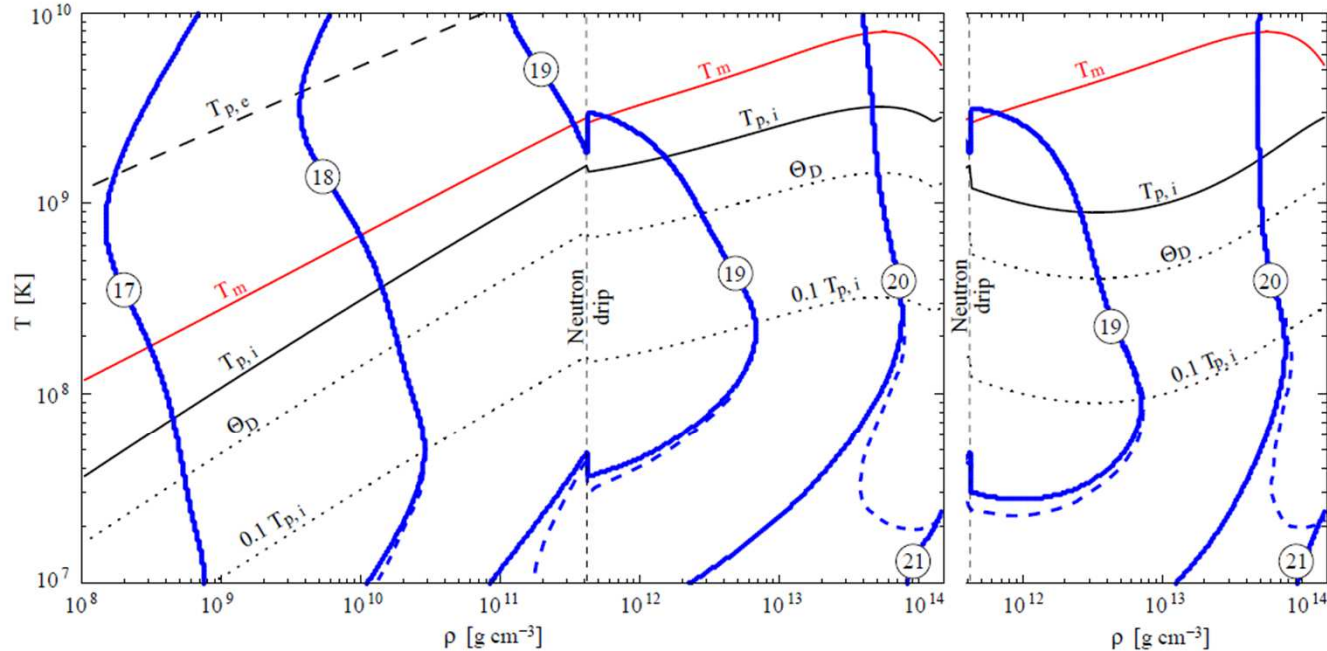
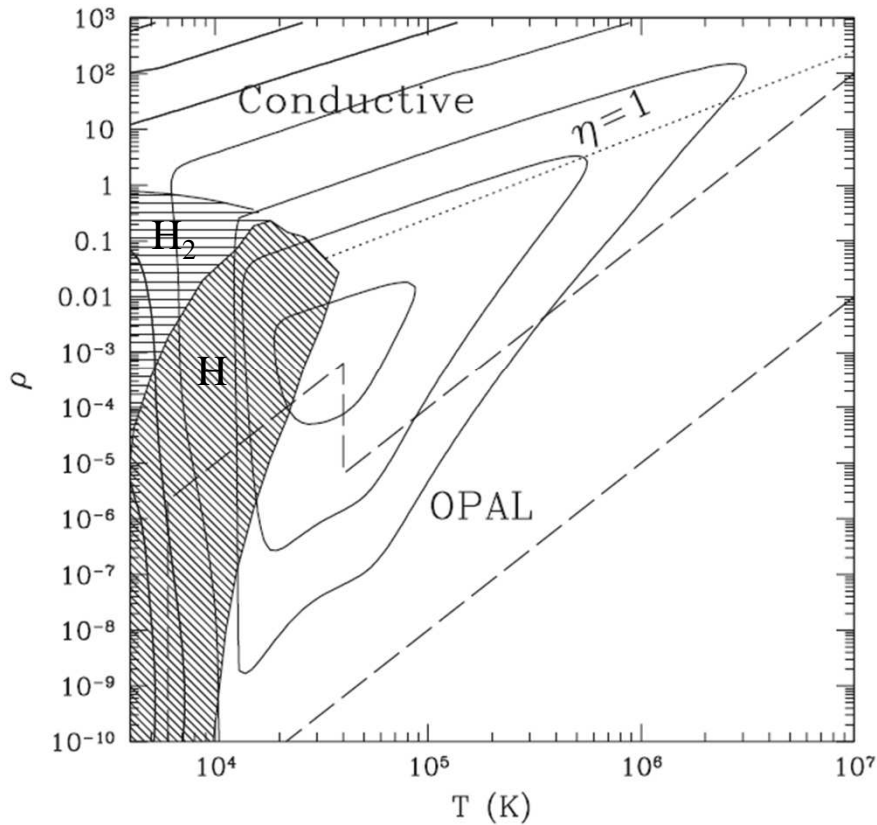


Fig. 4 Iso-contour lines of the electron thermal conductivity κ_e in the crust, labeled by the value of $\log_{10}(\kappa_e/\text{ergs}^{-1} \text{cm}^{-1} \text{K}^{-1})$, using the results of [Gnedin et al. \(2001\)](#). Also shown are the melting curve T_m , the electron and ion plasma temperatures, $T_{p,e}$ and T_p respectively, the Debye temperature, $\Theta_D \simeq 0.45T_p$, that marks the transition from classical to quantum solid and $0.1T_p$ below which the wholly quantum crystal regime is realized. The crust composition is the same as in [Fig. 2](#). The right panel only displays the inner crust but assuming that about 80% of the dripped neutrons are entrained: the strong reduction of T_p and Θ_D pushes the onset of the wholly quantum regime to lower T . The dashed contour lines illustrate the reduction of κ_e from impurity scattering, assuming an impurity parameter $Q_{\text{imp}} = 1$.

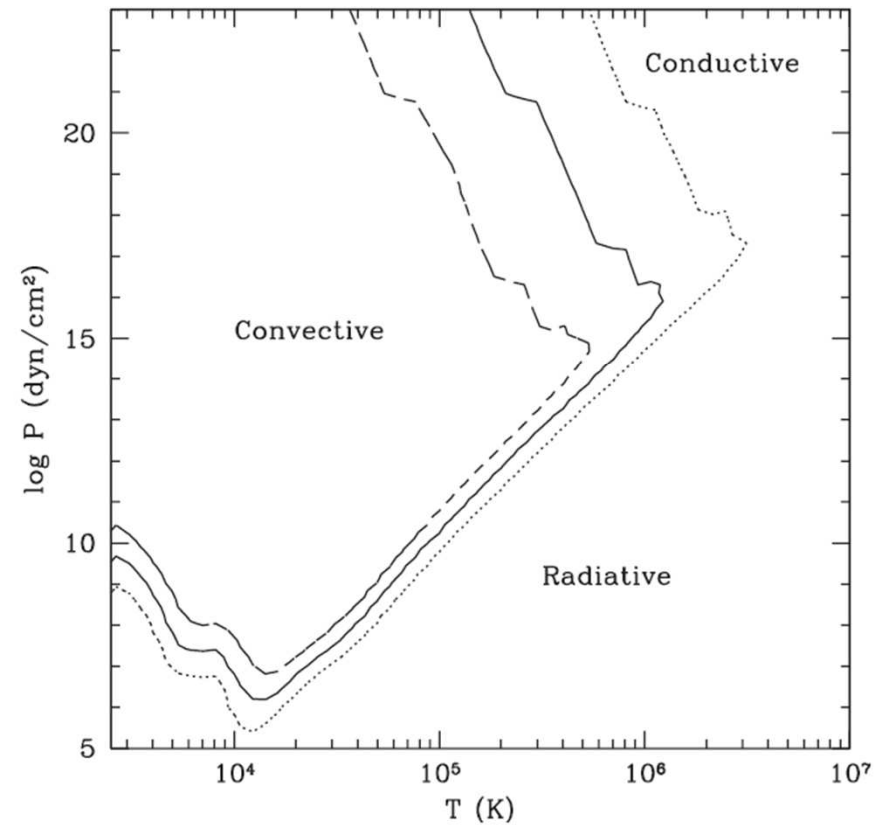
Теплоизолирующие оболочки белого карлика

B. Hansen / Physics Reports 399 (2004) 1–70



Непрозрачности

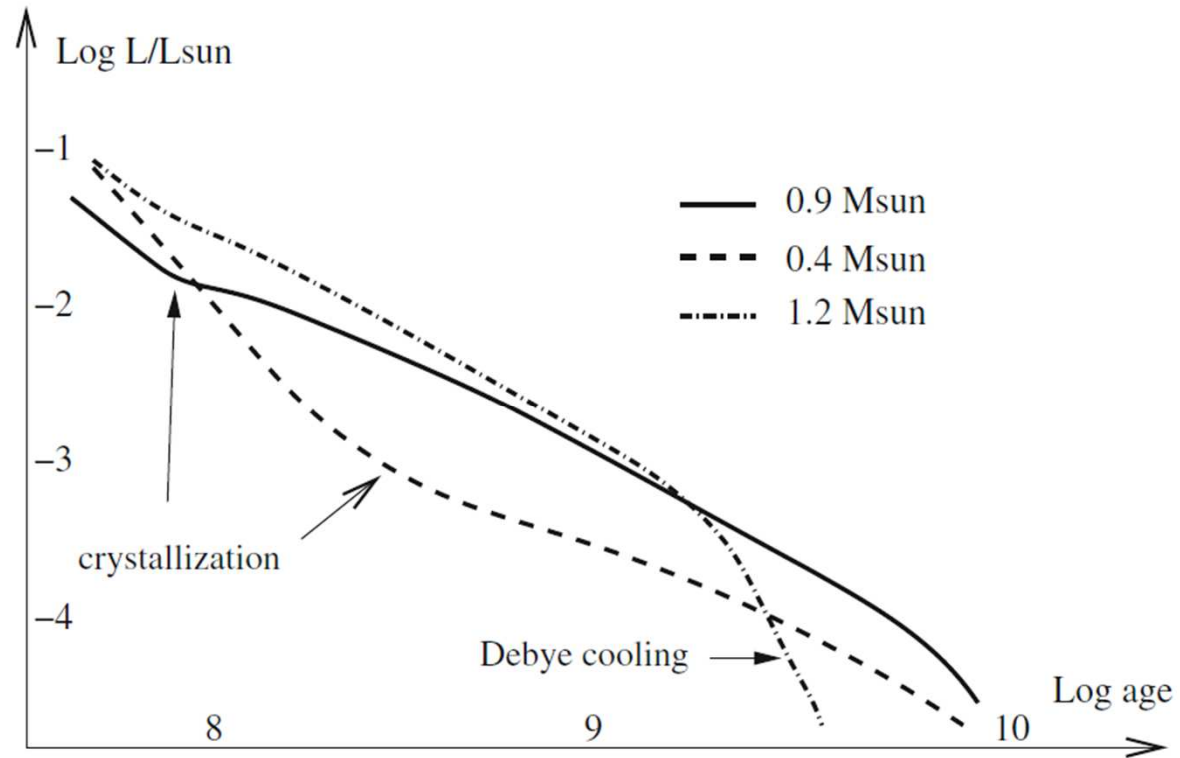
B. Hansen / Physics Reports 399 (2004) 1–70



Доминирующие процессы теплопереноса
(разные контуры – для разных светимостей)

Остывание белого карлика

с учётом кристаллизации ядра и дебаевского подавления теплоёмкости при низких температурах



Surface luminosity as a function of cooling time for white dwarfs with a carbon core

Рисунок из обзора: Althaus et al., *Astron. Astrophys. Rev.* **18**, 471–566 (2010)

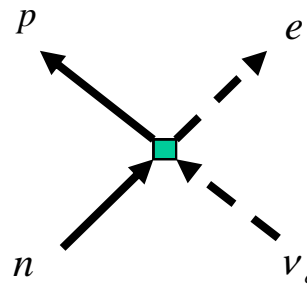
Нейтринное излучение

Урка-процессы

$$n \rightarrow p + e + \bar{\nu}_e, \quad p + e \rightarrow n + \nu_e$$



$$n \rightarrow n + \bar{\nu}_e + \nu_e$$



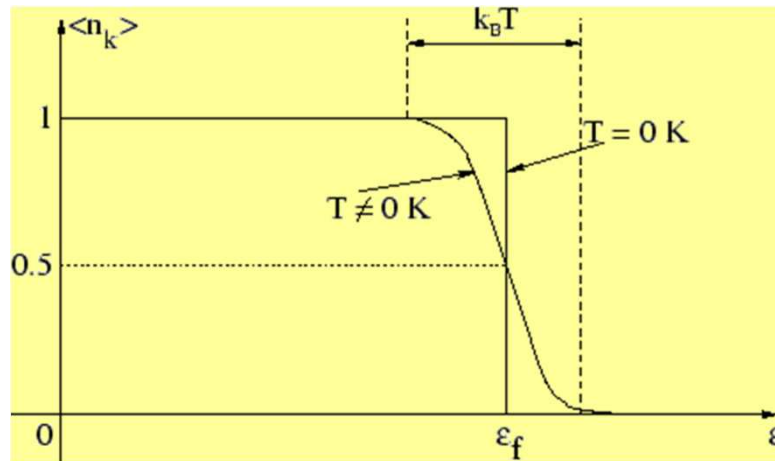
Г.А.Гамов (1904-1968)



М.Шёнберг (1916-1990)

$$Q \sim 3 \times 10^{27} T_9^6 \text{ erg cm}^{-3} \text{ s}^{-1}$$

$$L_\nu \sim 10^{46} T_9^6 \text{ erg s}^{-1}$$



Порог: $p_{Fn} \leq p_{Fp} + p_{Fe}$

$$\rho \geq 2\rho_0, \text{ где } \rho_0 = 2,8 \times 10^{14} \text{ г/см}^3.$$

Модифицированные урка («мурка») процессы:

$$N + n \rightarrow N + p + e + \bar{\nu}_e, \quad N + p + e \rightarrow N + n + \nu_e$$

Нейтринное излучение


D.G.Yakovlev *et al.*, “Neutrino emission from neutron stars”, *Phys.Rep.* **354**, 1 (2001)

Во внутреннем ядре достаточно массивной нейтронной звезды:

нуклоны, гипероны	$n \rightarrow p + e + \nu_e$ $p + e \rightarrow n + \nu_e$	$Q \sim 3 \times 10^{27} T_9^6 \frac{\text{erg}}{\text{cm}^3 \text{s}}$	$L_\nu \sim 10^{46} T_9^6 \frac{\text{erg}}{\text{s}}$
пионный конденсат	$\tilde{n} \rightarrow \tilde{p} + e + \nu_e$ $\tilde{p} + e \rightarrow \tilde{n} + \nu_e$	$Q \sim 10^{24-26} T_9^6 \frac{\text{erg}}{\text{cm}^3 \text{s}}$	$L_\nu \sim 10^{42-44} T_9^6 \frac{\text{erg}}{\text{s}}$
каонный конденсат	$\tilde{n} \rightarrow \tilde{p} + e + \nu_e$ $\tilde{p} + e \rightarrow \tilde{n} + \nu_e$	$Q \sim 10^{23-24} T_9^6 \frac{\text{erg}}{\text{cm}^3 \text{s}}$	$L_\nu \sim 10^{41-42} T_9^6 \frac{\text{erg}}{\text{s}}$
кварки	$d \rightarrow u + e + \nu_e$ $u + e \rightarrow d + \nu_e$	$Q \sim 10^{23-24} T_9^6 \frac{\text{erg}}{\text{cm}^3 \text{s}}$	$L_\nu \sim 10^{41-42} T_9^6 \frac{\text{erg}}{\text{s}}$

Во всём ядре (почти любой) нейтронной звезды:

«мурка»- процессы	$n + N \rightarrow p + e + N + \nu_e$ $p + e + N \rightarrow n + N + \nu_e$	$Q \sim 10^{20-22} T_9^8 \frac{\text{erg}}{\text{cm}^3 \text{s}}$	$L_\nu \sim 10^{38-40} T_9^8 \frac{\text{erg}}{\text{s}}$
Тормозное излучение	$N + N \rightarrow N + N + \nu + \bar{\nu}$	$Q \sim 10^{18-20} T_9^8 \frac{\text{erg}}{\text{cm}^3 \text{s}}$	$L_\nu \sim 10^{36-38} T_9^8 \frac{\text{erg}}{\text{s}}$


 ν_e, ν_μ, ν_τ

Нейтринное излучение

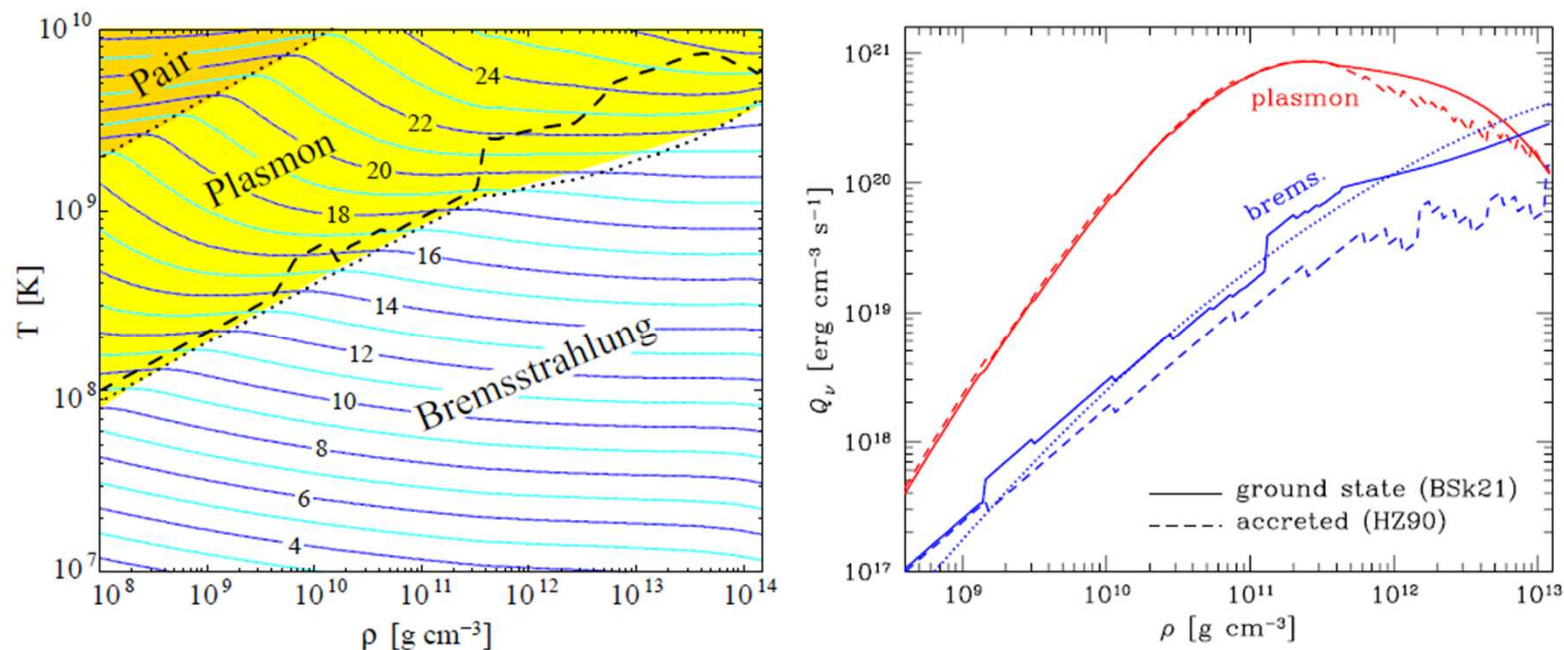


Fig. 3 Neutrino emissivity Q_ν in a non-magnetized crust from the pair annihilation, plasmon decay, and electron-ion bremsstrahlung processes. Left panel: The contour lines are labeled by the value of $\log_{10}[Q_\nu/(\text{erg cm}^{-3} \text{ s}^{-1})]$. Regions where the pair, plasma, and bremsstrahlung processes dominate are indicated: the boundaries happen to be quite well described by the two dotted lines that show $\frac{5}{3}T_{p,e}$ and $\frac{1}{13}T_{p,e}$. (Also indicated is the ion melting curve, dashed line.) Right panel: Density dependences of Q_ν for the ground-state nuclear matter (solid lines) and for the accreted crust (dashed lines) at $T = 10^9$ K. The dotted line represents an older fit to the bremsstrahlung process (see text for detail).

Рисунок из обзора: Potekhin et al., *Space Sci. Rev.* **191**, 239 (2015)

Остывание белого карлика

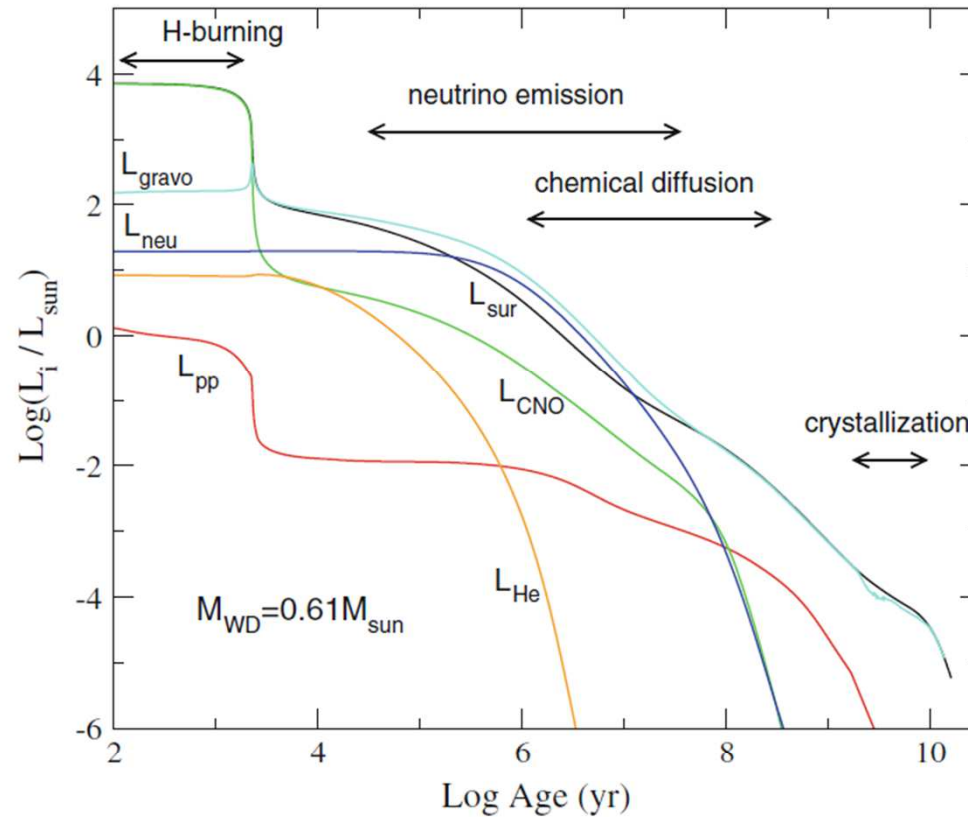


Figure 10. Time dependence of the different luminosity contributions for a $0.61 M_{\odot}$ white dwarf: photon luminosity, L_{sur} ; luminosity due to nuclear reactions (proton–proton, L_{pp} , CNO bicycle, L_{CNO} , He burning, L_{He}); neutrino losses, L_{neu} ; and rate of gravothermal (compressional plus thermal) energy release L_{gravo} . The white dwarf progenitor corresponds to an initially $2 M_{\odot}$ star with metallicity $Z = 0.01$. Calculations include element diffusion, release of latent heat upon crystallization, and outer boundary conditions as given by nongray model atmospheres. The different physical processes of relevance during white dwarf evolution are indicated

Профили температуры в нейтронной звезде

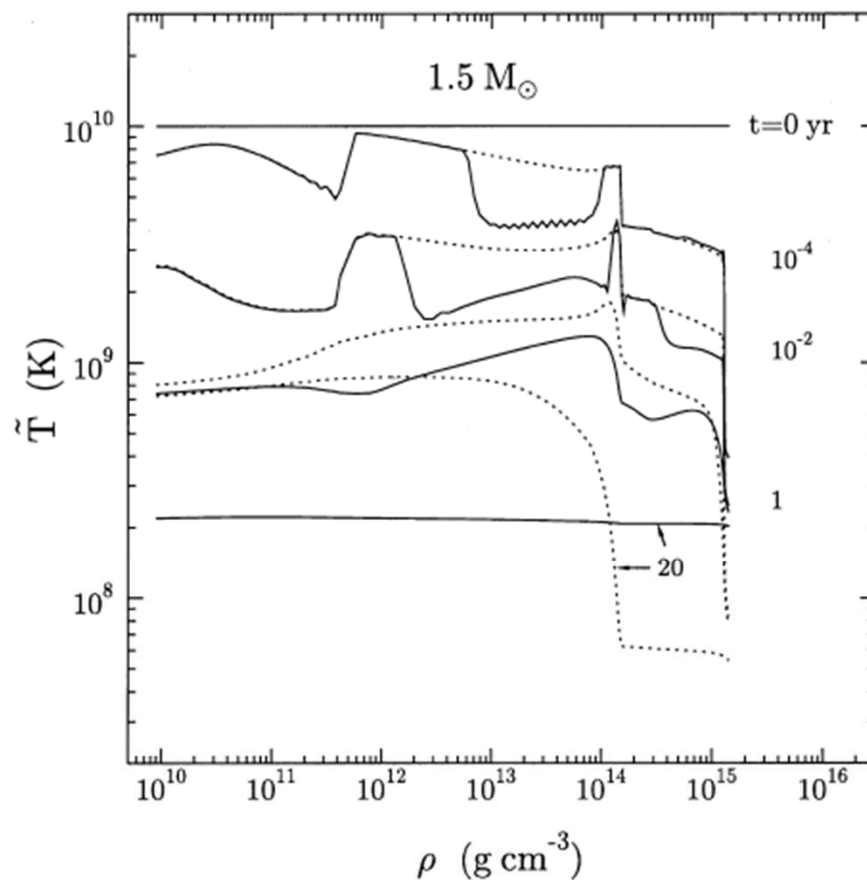


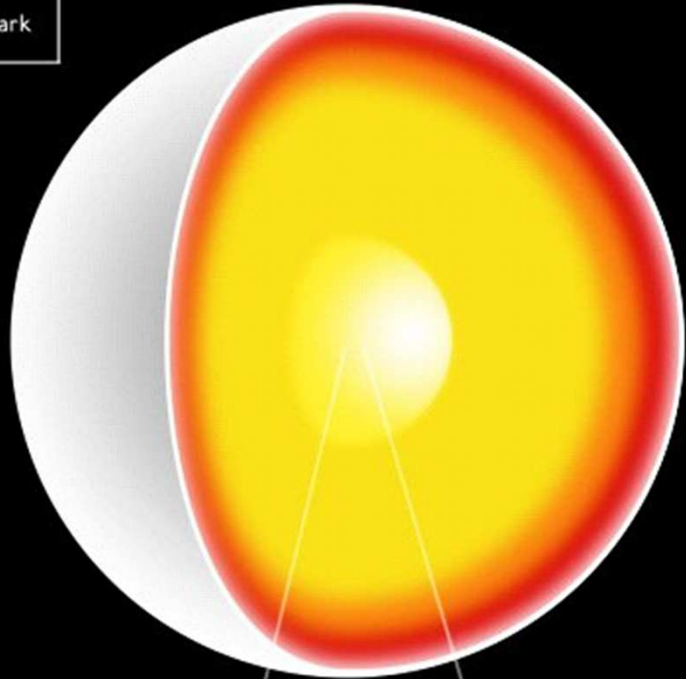
Figure 13. Temperature profiles (solid lines) in the interior of the $1.5\text{-}M_{\odot}$ model with strong superfluidity both in the crust and the core. The numbers next to the curves show the stellar age. The contours are at 0, 10^{-4} , 10^{-2} , 1 and 20 yr. The dotted lines show the temperature profiles of the non-superfluid star.

Рисунок из статьи: Gnedin et al., *MNRAS* **324**, 725 (2001)

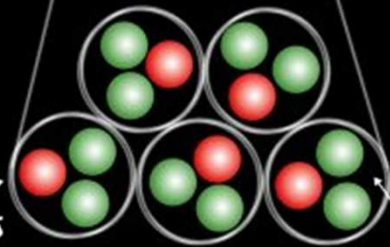
Кварковые звёзды

- Up Quark
- Down Quark
- Strange Quark

Neutron Star

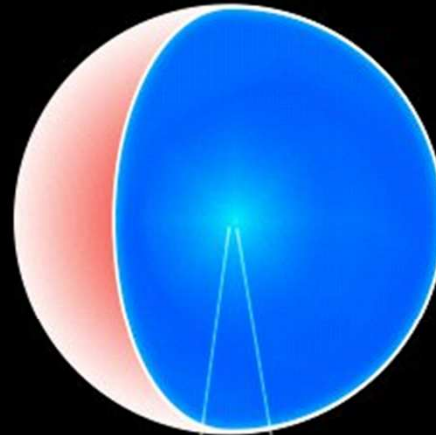


NEUTRONS



CONFINED QUARKS

Strange Quark Star



FREE QUARKS

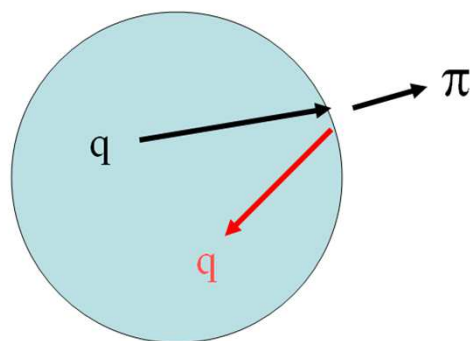
Кварковые звёзды

Кварковые урка-процессы – быстрое остывание:

$$d \rightarrow u + e^- + \bar{\nu}_e$$

$$u + e^- \rightarrow d + \nu_e$$

Сильное электрическое поле у поверхности; образование π -мезонов и пар e^-e^+ – быстрое остывание:



$$\pi^0 \rightarrow 2\gamma \leftrightarrow e^+e^-$$

$$\pi^\pm \rightarrow \mu^\pm + \nu_\mu$$

$$\mu^\pm \rightarrow e^\pm + \nu_e + \nu_\mu$$

Кварковые звёзды

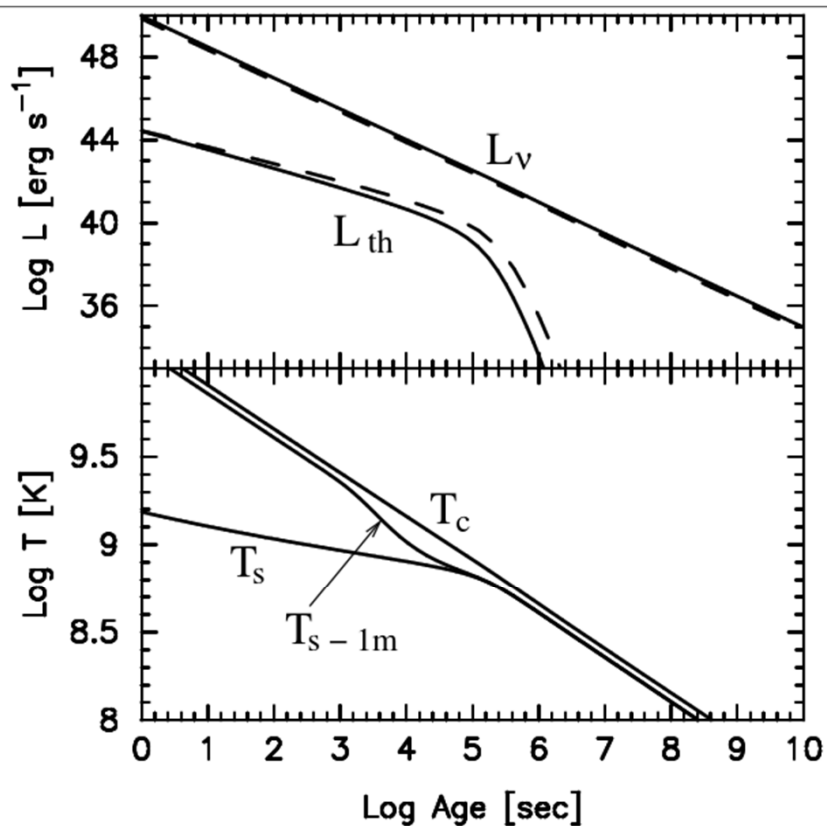


FIG. 1: Upper panel: luminosities in neutrinos, L_ν , and photons plus e^+e^- pairs, L_{th} , for a strange star in the normal phase (solid lines) and in the 2SC phase (dashed lines). Lower panel: temperature in the center, T_c , at the surface, T_s , and 1 meter below the surface, T_{s-1m} of the strange star in the normal phase. The large difference between T_s and T_{s-1m} at early times illustrates the enormous temperature gradient present just below the surface because of the large L_{th} .